Inorg. Chem. **2004**, *43*, 5676–5680

Hydrothermal Synthesis, Crystal Structure, Conductivity, and Thermal Decomposition of $[Cu(4,4'\text{-bipy})(H_2O)(Mo_3O_{10})]\cdot H_2O$

Zuping Kong, Linhong Weng, Dejun Tan, Heyong He, Biao Zhang, Jilie Kong, and Bin Yue*

Department of Chemistry and Shanghai Key Laboratory of Molecular Catalysis and Innovative Materials, Fudan University, Shanghai 200433, China

Received March 23, 2004

The hydrothermal reaction of $(NH_4)_6Mo_7O_{24}\cdot 4H_2O$, $CuCl_2\cdot 2H_2O$, and 4,4′-bipyridine yields bipyridine-ligated copper-trimolybdate monohydrate $[Cu(4,4'\text{-bipy})(H_2O)(Mo_3O_{10})]\cdot H_2O$ in the monoclinic system with space group of $C_{2/c}$ and cell parameters of $a = 15.335(2)$ Å, $b = 15.535(2)$ Å, $c = 15.106(2)$ Å, $\beta = 101.162(2)°$, $V = 3530.7(9)$ Å^3, and $Z = 8$. Its structure consists of one-dimensional infinite $\{[Mo_3O_{10}]^{2-}\}_\infty$ chains linked through $\{Cu_2(H_2O)_2(4,4'\text{-bipy})\}$ units. The Mo–O chain contains distorted $\{MoO_6\}$ octahedra connected through corner-sharing oxygen atoms into infinite chains along the *c* direction and each chain is located in the channel formed by four adjacent crossing chains of $\{Cu(4,4'\text{-bipy})(H_2O)\}_n^{2n+}$. The crystal shows weak conductivity through Mo–O chain along the *c* direction and insulating property along either *a* or *b* direction. Furthermore, a crystalline bimetallic oxide, $CuMo_3O_{10}$, forms when the title compound undergoes thermal treatment in N_2 atmosphere after the complete removal of the ligands.

Introduction

Hybrid organic−inorganic materials have become a major research theme in inorganic and materials chemistry.[1] The synergistic interaction between organic and inorganic component leads to complex compositions and diverse structures of the materials, and these materials usually show unusual features and multifunctionalities.[2] The synthetic strategies for controlling structure−function relationship have been extensively investigated by focusing on the property of the diphasic interface and the structural directing role of organic compounds.[3] According to the nature of the bonds between organic and inorganic components, the materials can be divided into two major families in which one exhibits weak bonding while another exhibits strong bonding. The former has been exploited for preparation of some important materials such as zeolites[4] and mesoporous materials[5] where the organic component (template) can be totally removed by facile calcination or extraction. The latter has also been applied for preparation of hybrids such as biomineralized materials,[6] microporous transition metal phosphates with entrained organic cations,[7] and molybdenum or vanadium oxide subunits modified by organonitrogen ligands or their coordinated metal cations where the framework is usually sustained by the organic component.[8]

Currently, molybdenum polyoxoanions attract much attention due to their versatile stoichiometry, different structure, and high reactivity. The exploration of a generalized approach for preparation of one-, two-, and three-dimensional organodiamine-templated molybdenum oxides and hybrid

* Author to whom correspondence should be addressed. Tel: 86-21-65642779. Fax: 86-21-65338041. E-mail: yuebin@fudan.edu.cn.

(1) Forster, P. M.; Thomas, P. M.; Cheetham, A. K. *Chem. Mater.* **2002**, *14*, 17.
(2) Stupp, S. I.; Braun, P. V. *Science* **1997**, *277*, 1242.
(3) (a) Burkholder, E.; Golub, V.; O'Connor, C. J.; Zubieta, J. *Inorg. Chem.* **2003**, *42*, 6729. (b) Davis, M. E.; Katz, A.; Ahmad, W. R. *Chem. Mater.* **1996**, *8*, 1820. (c) Rarig, R. S., Jr.; Lam, R.; Zavalij, P. Y.; Ngala, J. K.; LaDuca, R. L., Jr.; Greedan, J. E.; Zubieta, J. *Inorg. Chem.* **2002**, *41*, 2124.
(4) (a) Smith, J. V. *Chem. Rev.* **1988**, *88*, 149. (b) Occelli, M. L.; Robson, H. C. *Zeolite Synthesis*; American Chemical Society: Washington, DC, 1989.
(5) Kresge, C. T.; Leonowicz, M. E.; Roth, W. J.; Vartuli, J. C.; Beck, J. S. *Nature* **1992**, *359*, 710.
(6) Mann, S. *Nature* **1993**, *365*, 499.
(7) (a) Haushalter, R. C.; Mundi, L. A. *Chem. Mater.* **1992**, *4*, 31. (b) Khan, M. I.; Meyer, L. M.; Haushalter, R. C.; Schweitzer, C. L.; Zubieta, J.; Dye, J. L. *Chem. Mater.* **1996**, *8*, 43.

10.1021/ic049608p CCC: $27.50
Published on Web 08/04/2004

bimetallic oxides using hydrothermal methods reported by Zubieta et al. and others further demonstrates the wide variety of molybdenum oxoanion subunits ranging from $\{MoO_4\}^{2-}$ to $\{Mo_8O_{26}\}^{4-}$, the existence of infinite chains of $\{MoO_6\}$ octahedra with different connecting modes linked through corner-, edge-, and/or face-sharing octahedra, and the influences of ligand and the coordination of metal if containing the secondary metal on the structural change.[9,10] In this study, we choose 4,4′-bipyridine (4,4′-bipy) as a polyfunctional rodlike ligand and copper as a secondary metal to hydrothermally synthesize bipyridine-ligated copper-trimolybdate monohydrate $[Cu(4,4'\text{-bipy})(H_2O)(Mo_3O_{10})]\cdot H_2O$. The crystal structure, conductivity, and thermal decomposition of the title compound are also reported.

Experimental Section

Synthesis of $[Cu(4,4'\text{-bipy})(H_2O)(Mo_3O_{10})]\cdot(H_2O)$. A mixture of $(NH_4)_6Mo_7O_{24}\cdot 4H_2O$, $CuCl_2\cdot 2H_2O$, and 4,4′-bipy in H_2O with a molar ratio of 1:2:2:1110 in an autoclave was heated at 150 °C for two weeks under autogenous pressure. After the reaction, the autoclave was slowly cooled to room temperature. Blue crystals in ca. 10% yield were obtained and washed with water. The excess starting materials remained in the solution as unknown species. IR spectrum of the crystal using KBr pellet exhibits intense bands at 490, 658 cm^{-1}, and 820, 887, 918, and 933 cm^{-1} assigned to ν(Mo−O−Mo) and ν(Mo═O), respectively,[11] and bands at 1620, 1540, 1420, and 1320 cm^{-1} assigned to characteristic vibrational modes of 4,4′-bipyridine.[12]

X-ray Crystallography. The single crystal of the title compound with dimensions of $0.25 \times 0.10 \times 0.05$ mm^3 was carefully selected under an optical microscope and glued to a thin glass fiber with epoxy resin. Crystal structure determination by X-ray diffraction was performed on a Bruker AXS SMART CCD diffractometer equipped with a normal-focus, 2.4-kW, sealed-tube X-ray source with Mo Kα radiation ($\lambda = 0.71073$ Å) operating at 50 kV and 30 mA. About 1.3-hemispheres of intensity data were collected at room temperature with a scan width of 0.30° in ω and an exposure time of 30 s per frame. The empirical absorption corrections were based on the equivalent reflections. The structure was solved by direct methods followed by successive difference Fourier methods. All calculations were performed using SHELXTL and SHELXTL-97,[13] and final full-matrix refinements were against F^2.

The crystal data, intensity collection, and structural refinement are summarized in Table 1. The selected interatomic distances and bond angles are given in Table 2. Crystallographic data (including structure factors) have been deposited at the Cambridge Crystallographic Data Centre (CCDC 212770).

Conductivity Measurement. The conductivity was measured at room temperature with a CHI600 Electrochemical Workstation (CH Instrument). The single crystal was connected to a pair of gold electrodes with silver conductive adhesive along with desired crystal axis.

Table 1. Summary of Crystallographic Data for the Structure of $[Cu(4,4'\text{-bipy})(H_2O)(Mo_3O_{10})]\cdot H_2O$

empirical formula	$C_{10}H_{12}CuMo_3N_2O_{12}$
fw	703.58
cryst syst	monoclinic
space group	$C_{2/c}$
a, Å	15.335(2)
b, Å	15.535(2)
c, Å	15.106(2)
β, deg	101.162(2)
V, Å^3	3530.7(9)
Z	8
D_{calcd}, gcm^{-3}	2.647
μ, cm^{-1}	33.38
no. of reflns	3849
λ, Å	0.71073
R1[a]	0.0249
wR2[b]	0.0487

[a] $R1 = \sum|F_o| - |F_c|/\sum|F_o|$. [b] $wR2 = \{\sum[w(F_o^2 - F_c^2)^2]/\sum[w(F_o^2)^2]\}^{1/2}$.

Table 2. Selected Bond Lengths (Å) and Angles (°) for $[Cu(4,4'\text{-bipy})(H_2O)(Mo_3O_{10})]\cdot H_2O$[a]

Mo1−O1	1.750(2)	Mo3−O6^{ii}	2.212(2)
Mo1−O2	1.905(2)	Mo3−O8	1.719(2)
Mo1−O3	1.973(2)	Mo3−O8^{ii}	1.719(2)
Mo1−O4	2.120(2)	Mo4−O2	2.277(2)
Mo1−O4^{i}	2.263(2)	Mo4−O3^{i}	2.220(2)
Mo1−O5	1.690(2)	Mo4−O4^{i}	1.951(2)
Mo2−O2	1.962(2)	Mo4−O6^{ii}	1.931(2)
Mo2−O2^{ii}	1.962(2)	Mo4−O9	1.709(2)
Mo2−O6	2.215(2)	Mo4−O10	1.708(2)
Mo2−O6^{ii}	2.215(2)	Cu5−O1	1.981(2)
Mo2−O7	1.696(2)	Cu5−O8^{v}	2.324(2)
Mo2−O7^{ii}	1.696(2)	Cu5−O11	1.977(3)
Mo3−O3^{i}	1.941(2)	Cu5−N1	1.949(3)
Mo3−O3^{iv}	1.941(2)	Cu5−N2^{vi}	1.974(3)
Mo3−O6	2.212(2)		
O1−Mo1−O2	100.5(1)	O3^{iv}−Mo3−O6	73.0(1)
O1−Mo1−O3	89.0(1)	O3^{iv}−Mo3−O6^{ii}	90.7(1)
O1−Mo1−O4	158.2(1)	O3^{iv}−Mo3−O8	91.5(1)
O1−Mo1−O4^{i}	91.9(1)	O3^{iv}−Mo3−O8^{ii}	100.9(1)
O1−Mo1−O5	102.9(1)	O6−Mo3−O6^{ii}	73.7(1)
O2−Mo1−O3	159.5(1)	O6−Mo3−O8	159.0(1)
O2−Mo1−O4	91.7(1)	O6−Mo3−O8^{ii}	92.9(1)
O2−Mo1−O4^{i}	74.3(1)	O6^{ii}−Mo3−O8	92.9(1)
O2−Mo1−O5	96.8(1)	O6^{ii}−Mo3−O8^{ii}	159.0(1)
O3−Mo1−O4	74.1(1)	O8−Mo3−O8^{ii}	104.0(2)
O3−Mo1−O4^{i}	87.3(1)	O2−Mo4−O3^{i}	77.7(1)
O3−Mo1−O5	98.8(1)	O2−Mo4−O4^{i}	73.2(1)
O4−Mo1−O4^{i}	74.0(1)	O2−Mo4−O6^{ii}	73.5(1)
O4−Mo1−O5	93.5(1)	O2−Mo4−O9	87.1(1)
O4^{i}−Mo1−O5	164.1(1)	O2−Mo4−O10	169.0(1)
O2−Mo2−O2^{ii}	157.2(1)	O3^{i}−Mo4−O4^{i}	72.2(1)
O2−Mo2−O6	87.3(1)	O3^{i}−Mo4−O6^{ii}	73.0(1)
O2−Mo2−O6^{ii}	74.4(1)	O3^{i}−Mo4−O9	164.7(1)
O2−Mo2−O7	94.9(1)	O3^{i}−Mo4−O10	91.4(1)
O2−Mo2−O7^{ii}	99.0(1)	O4^{i}−Mo4−O6^{ii}	73.0(1)
O2^{ii}−Mo2−O6	74.4(1)	O4^{i}−Mo4−O9	103.2(1)
O2^{ii}−Mo2−O6^{ii}	87.3(1)	O4^{i}−Mo4−O10	103.8(1)
O2^{ii}−Mo2−O7	99.0(1)	O6^{ii}−Mo4−O9	103.1(1)
O2^{ii}−Mo2−O7^{ii}	94.9(1)	O6^{ii}−Mo4−O10	103.4(1)
O6−Mo2−O6^{ii}	73.6(1)	O9−Mo4−O10	103.9(1)
O6−Mo2−O7	91.7(1)	O1−Cu5−O8^{v}	88.1(1)
O6−Mo2−O7^{ii}	161.9(1)	O1−Cu5−O11	179.2(1)
O6^{ii}−Mo2−O7	161.9(1)	O1−Cu5−N1	88.4(1)
O6^{ii}−Mo2−O7^{ii}	91.7(1)	O1−Cu5−N2^{vii}	91.0(1)
O7−Mo2−O7^{ii}	104.6(2)	O8^{v}−Cu5−O11	91.1(1)
O3^{i}−Mo3−O3^{iv}	159.8(1)	O8^{v}−Cu5−N1	97.6(1)
O3^{i}−Mo3−O6	90.7(1)	O8^{v}−Cu5−N2^{vi}	94.7(1)
O3^{i}−Mo3−O6^{ii}	73.0(1)	O11−Cu5−N1	91.8(1)
O3^{i}− Mo3−O8	100.9(1)	O11−Cu5−N2^{vi}	89.0(1)
O3^{i}−Mo3−O8^{iv}	91.5(1)	N1−Cu5−N2^{vi}	167.6(1)

[a] Symmetry transformations used to generate equivalent atoms: (*i*) $-x + 2, -y, -z + 1$; (*ii*) $-x + 2, y, -z + 3/2$; (*iii*) $x - 1/2, y - 1/2, z$; (*iv*) $x, -y, z + 1/2$; (*v*) $x, -y, z - 1/2$; (*vi*) $x + 1/2, y + 1/2, z$; (*vii*) $x - 1/2, -y + 1/2, z - 1/2$; (*viii*) $-x + 3/2, -y + 1/2, -z + 1$; (*viiii*) $-x + 1, y, -z + 1/2$; (*x*) $= -x + 1, -y, -z + 1$.

(8) (a) Hagrman, D.; Zubieta, C.; Rose, D. J.; Zubieta, J.; Haushalter, R. C. *Angew. Chem., Int. Ed. Engl.* **1997**, *36*, 873. (b) Hagrman, D.; Hagrman, P.; Zubieta, J. *Inorg. Chim. Acta* **2000**, *300*, 212. (c) Zhang, Y. P.; DeBord, J. R. D.; O'Connor, C. J.; Haushalter, R. C.; Clearfield, G.; Zubieta, J. *Angew. Chem., Int. Ed. Engl.* **1996**, *35*, 989. (d) DeBord, J. R. D.; Zhang, Y. P.; Haushalter, R. C.; Zubieta, J.; O'Connor, C. J. *J. Solid State Chem.* **1996**, *122*, 251. (e) Hagrman, P. J.; Zubieta, J. *Inorg. Chem.* **2001**, *40*, 2800.

(9) Hagrman, P. J.; Hagrman, D.; Zubieta, J. *Angew. Chem., Int. Ed. Engl.* **1999**, *38*, 2639.

(10) Xu, Y.; An, L. H.; Koh, L. L. *Chem. Mater.* **1996**, *8*, 814.

(11) Khan, M. I.; Chen, Q.; Zubieta, J. *Inorg. Chim. Acta* **1993**, *213*, 325.

(12) Strukl, J. S.; Walter, J. L. *Spectrochim. Acta* **1971**, *27A*, 223.

(13) (a) Sheldrick, G. M. *Acta Crystallogr.*, **1990**, *A46*, 467. (b) Sheldrick, G. M. *SHELXL-90, Program for the Refinement of Crystal Structures*; University of Goettingen, Germany, 1997.

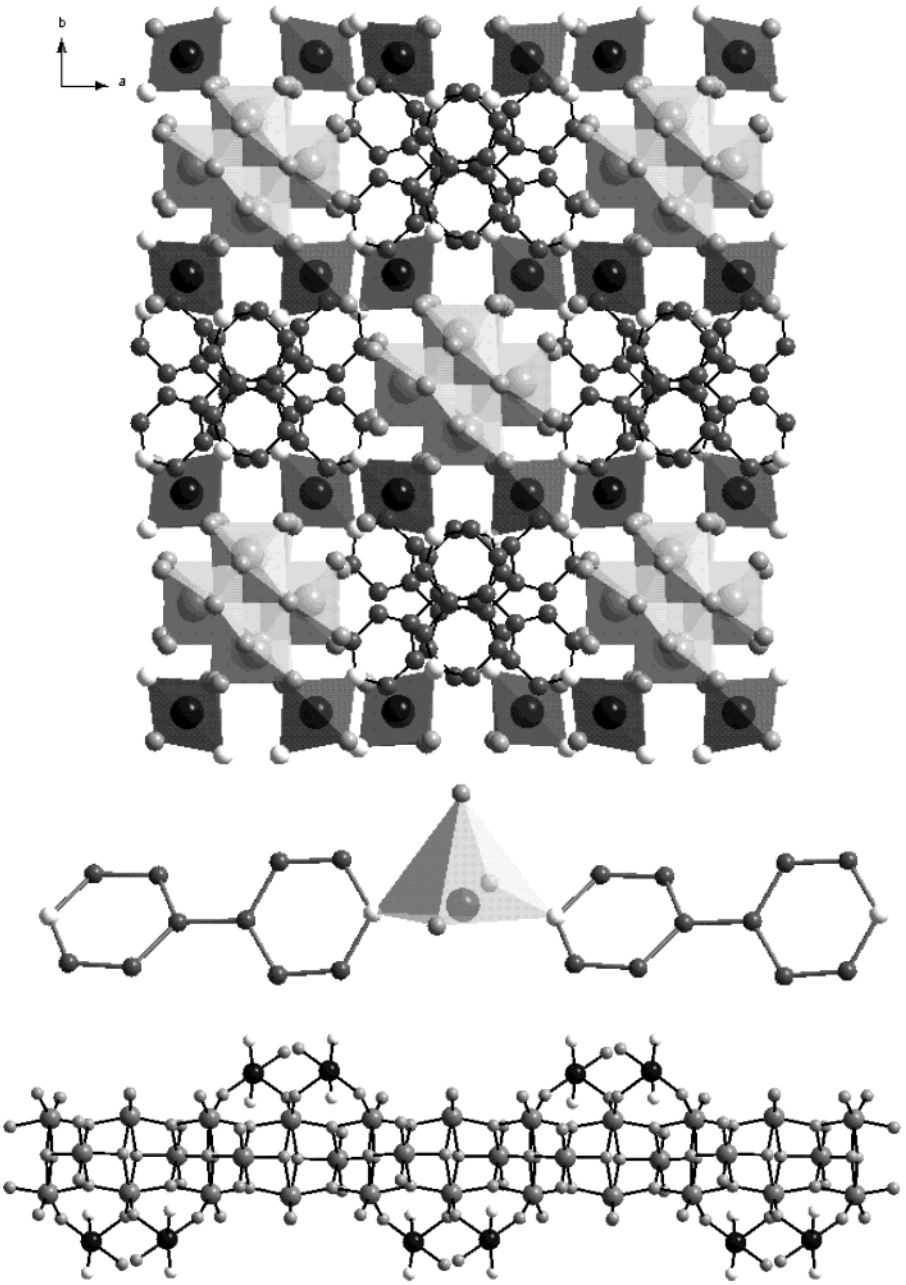

Figure 1. (a) View of the structure of $[Cu(4,4'\text{-bipy})(H_2O)(Mo_3O_{10})]\cdot H_2O$, along the *c* axis, illustrating the three-dimensional framework of $[Mo_3O_{10}]^{2-}$ chains incorporated within the scaffolding by $\{Cu(4,4\text{-bipy})\}_n^{2n+}$ subunits; (b) coordination sphere of the copper atom; and (c) a view of the $[Mo_3O_{10}]^{2-}$ chains and the appended {Cu(4,4-bipy)} groups which serve to bridge adjacent chains.

Thermogravimetric Analyses. Thermogravimetric measurement was performed on a Perkin-Elmer TGA7 thermogravimetric analyzer under a 100 mL/min flow of nitrogen in the 25−600 °C temperature range at a rate of 10 °C/min.

In Situ XRD Measurement under Programmed Temperature Treatment. XRD patterns of the sample were recorded on a Bruker D8 Advanced X-ray diffractometer using Cu Kα radiation with a voltage of 40 kV and a current of 40 mA. Variable-temperature in situ XRD experiment was carried out from room temperature to 600 °C at a rate of 0.2 °C/s.

Transmission Electron Microscopy (TEM). High-resolution TEM (HRTEM) and selected area electron diffraction (SAED) were performed using a Joel JEM-2010 transmission electron microscope. Elemental maps were obtained by energy-dispersive X-ray spectra analysis (EDX) of the K-edge fluorescence for Cu and Mo.

Results and Discussion

Structural Description. As shown in Figure 1a, the title compound is constructed from $[Mo_3O_{10}]^{2-}$ chains incorporated within the scaffolding by $\{Cu(4,4\text{-bipy})\}_n^{2n+}$ subunits. The structure consists of $\{CuO_3N_2\}$ square pyramids and $\{MoO_6\}$ octahedra, forming a three-dimensional bimetallic oxide framework with channels occupied by the 4,4′-bipy ligands. The cationic component forms one-dimensional chains of $\{CuO_3N_2\}$ square pyramid linked through bridging bidentate 4,4′-bipy groups. Each Cu^{II} site of the chain is coordinated to one H_2O molecule, two terminal oxo groups from the molybdate cluster subunit, and two nitrogen atoms from two 4,4′-bipy ligands to form slightly distorted square pyramidal coordination with one terminal O atom at the

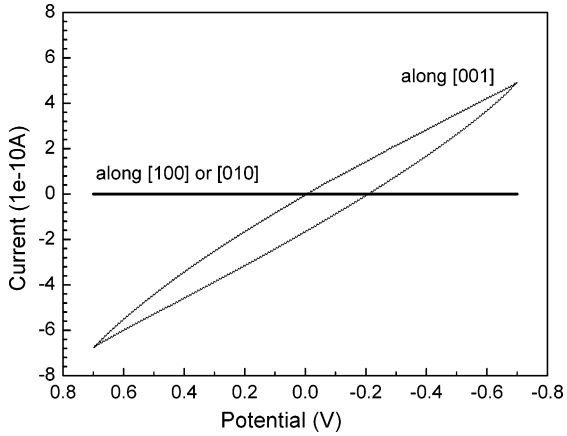

Figure 2. Conductivity of the title compound.

apical position (Figure 1b). The central Cu atom is displaced by 0.114(1) Å from the equatorial plane defined by N1, N2^{vi}, O1, and O11 atoms toward O8^{v}, and the Cu−N bond distances are 1.949 and 1.974 Å, while the axial Cu−O bond distance is 2.324 Å. The chains exhibit a 27.35° twist between the rings of the bipyridyl units. The two distinct chains along [110] and [001] directions form a right angle or virtual square network. When viewed along the *c* axis, the $\{Cu(4,4\text{-bipy})\}_n^{2n+}$ scaffoldings are linked through $\{CuO_3N_2\}$ square pyramid to produce channels of sufficient diameter to accommodate $[Mo_3O_{10}]^{2-}$ chains. As shown in Figure 1c, $\{MoO_6\}$ octahedra form a chain which is structurally analogous to that observed in the one-dimensional $(NH_4)[Mo_3O_{10}]$.[14] The infinite zigzag chains of $(Mo_3O_{10})^{2-}$ moiety stretch along the *c* axis, which is different from the case reported in the one-dimensional molybdenum oxide $[Cu_2(pyrd)(Mo_3O_{10})]$.[15]

Conductivity. The anisotropic properties of the $[Cu(4,4'\text{-bipy})(H_2O)(Mo_3O_{10})]\cdot H_2O$ single crystal can be proved by measuring the conductivity along the specific direction of crystal axis. The voltammetric curves along the *c* and *a* or *b* directions are shown in Figure 2. The conductivity of the single crystal is approximately 4.3×10^{-8} s cm^{-1} along the *c* direction and effectively zero along the *a* and *b* directions. Molybdenum−copper composite oxides have been of interest as a candidate for cathode materials in high-energy-density secondary batteries, and their conductivity is related to the content of copper, in which the oxide with the composition of $Cu_{0.3}MoO_3$ shows the highest conductivity, ca. 4.16×10^{-2} s cm^{-1}.[16] In the present case, the current passes through the $\{MoO_6\}$ octahedra chains along the *c* axis and the copper atoms do not involve in the electric conduction. Therefore, only the molybdenum−oxygen chains account for the weak conducting property whereas the copper−bipydine chains parallel to (001) are insulating.

Thermal Behavior. As shown in Figure 3, the thermal decomposition of the title compound under nitrogen exhibits

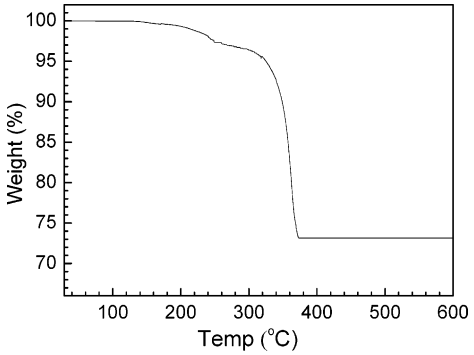

Figure 3. TG curve of the title compound.

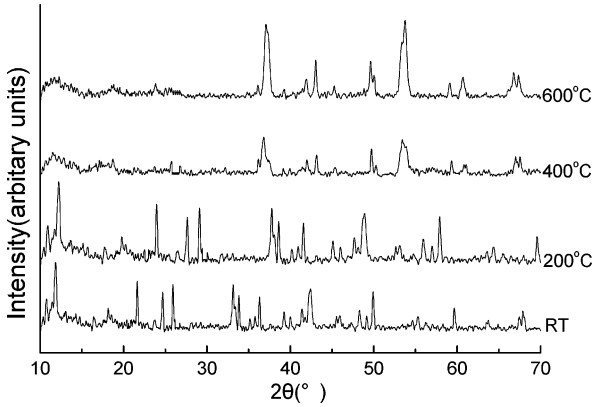

Figure 4. Variable-temperature in situ XRD patterns of the title compound.

a gradual dehydration in the range from room temperature to 250 °C, accounting for a 2.7% weight loss, which is attributed to the release of the crystalline water (2.56% theoretical weight loss). This process is followed by a consecutive weight loss of ca. 24.2%, which is attributed to the release of an aqua ligand and the decomposition of ligands (24.76%, theoretical weight loss) in the range of 250−370 °C. The mass becomes constant above 370 °C. The total weight loss of 26.9% is consistent with calculated value (27.32%) if $CuMo_3O_{10}$ is the final product. EDX result also indicates Cu/Mo molar ratio of 1:3 remains unchanged.

To understand the decomposition process and phase transition, temperature-dependent in situ XRD experiments of the title compound were acquired. In Figure 4 the pattern of the title compound at room temperature displays the characteristic diffraction peaks which can be indexed according to the crystal parameters of $[Cu(4,4'\text{-bipy})(H_2O)(Mo_3O_{10})]\cdot H_2O$. At 200 °C, the pattern shows some changes, indicating the variation of the structure due to the loss of water. The loss of the aqua ligand and the decomposition of bipydine took place between 200 and 400 °C with the appearance of a new set of diffraction peaks which can be indexed according to an orthorhombic phase with parameters of $a = 6.795$ Å, $b = 6.546$ Å, and $c = 4.285$ Å. These diffraction peaks are unchanged until 600 °C and remain upon cooling to room temperature. The found *d* values are consistent with those calculated from the cell parameters. HRTEM and SAED images provide further evidences to the new phase. SAED (Figure 5a) shows the nature of single

(14) Range, K.; Fässler, A. *Acta Crystallogr., Sect. C* **1990**, *46*, 488.
(15) Hagrman, D.; Warren, C. J.; Haushalter, R. C.; Seip, C.; O'Connor, C. J.; Rarig, R. S., Jr.; Johnson, K. M.; LaDuca, R. L., Jr.; Zubieta, J. *Chem. Mater.* **1998**, *10*, 3294.
(16) Tian, S. B.; Zhou, F.; Yang, J. C.; Li, Z. C. *Solid State Ionics* **1992**, *57*, 109.

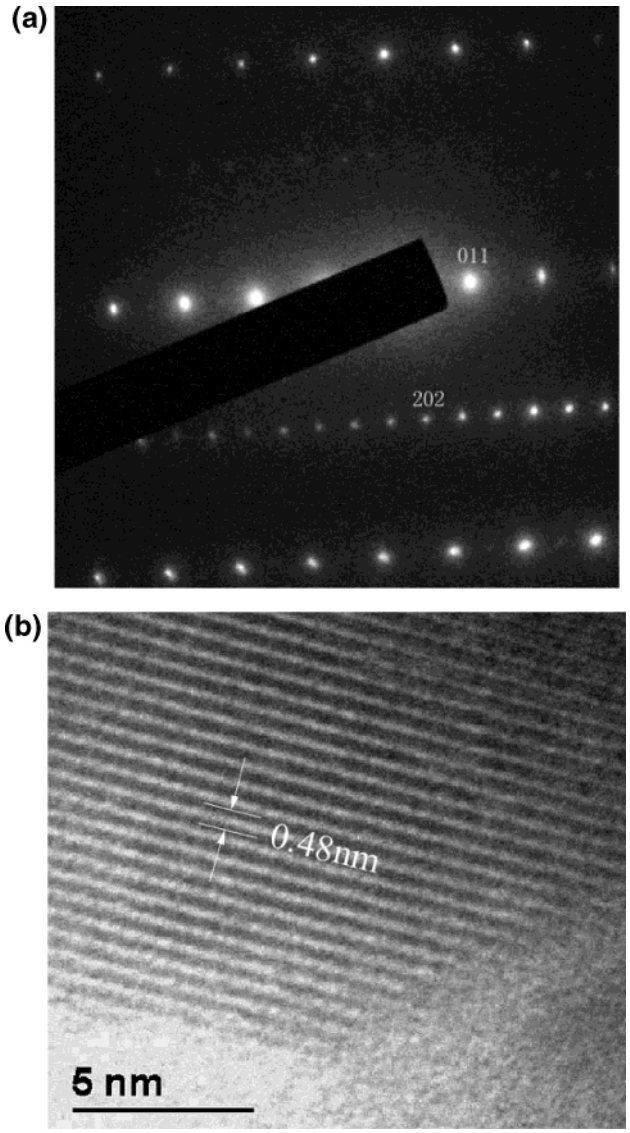

Figure 5. (a) SAED and (b) TEM images of the resulting product of $CuMo_3O_{10}$ after thermal decomposition of the title compound.

crystal. In a typical TEM image (Figure 5b), crystal lattice of Mo−Cu composite oxide shows that the distance between two fringes is ca. 0.48 nm compared with *d*-spacing of (110) in orthorhombic phase of $CuMo_3O_{10}$ and each particle shows the same crystalline orientation. To our knowledge, organoamine ligated bimetallic oxides generally undergo thermal decomposition to form unidentified phase, amorphous phase, or mixture, even though the copper trimolybdate hydrate ($CuMo_3O_{10}\cdot 5H_2O$) became amorphous under heating treatment.[17] Therefore, the present result indicates that thermal treatment of the hybrid organic−inorganic composite materials may break a new path to obtain crystalline bimetallic oxides.

Conclusions

The hydrothermal technique has been exploited to prepare a new hybrid organic−inorganic material of bipyridine-ligated copper-trimolybdate monohydrate [Cu(4,4′-bipy)-$(H_2O)(Mo_3O_{10})]\cdot H_2O$. The compound exhibits three-dimensional framework, which contains one-dimensional infinite $\{[Mo_3O_{10}]^{2-}$ chains located in the channel formed by four adjacent crossing chains of $\{Cu(4,4'\text{-bipy})(H_2O)\}_n^{2n+}$. The anisotropic property of the crystal has been observed by measuring conductivity of the crystal along different directions. The title compound undergoes thermal decomposition to form a new crystalline phase of a bimetallic oxide, $CuMo_3O_{10}$, which has been characterized by XRD, TEM and SAED.

Acknowledgment. This work was supported by the National Natural Sciences Foundation Committee of China (Grants 20371013 and 20005310), National Basic Research Program of China (2003CB615807), and Shanghai Science and Technology Committee (03DJ14004).

Supporting Information Available: X-ray crystallographic files, in CIF format, for title compound, and table giving index results of $CuMo_3O_{10}$ (pdf). This material is available free of charge via the Internet at http://pubs.acs.org.

IC049608P

(17) Surga, W. J.; Lasocha, W.; Hodorowicz, S. A. *Thermochim. Acta* **1998**, *317*, 193.